Mechanics and Mechanical Engineering
Vol. 17, No. 2 (2013) 157–166

Free Vibrations of Carbon Nanotubes with Defects

Aleksander Muc
Aleksander Banaś
Małgorzata Chwał
Institute of Machine Design
Cracow University of Technology
al. Jana Pawa II 37, 31–864 Cracow, Poland

Received (11 March 2013)
Revised (16 April 2013)
Accepted (20 May 2013)

In the paper the eigenfrequencies of pristine and defective single-walled carbon nanotubes are investigated. The defects are in the form of point vacancies. The axial vibrations of structures are studied only. A special attention is focused on the effects of material and geometrical properties of nanostructures on the results. Three different models are considered: the Euler beam model, a continuous specially orthotropic model and a 3D nonlinear finite element model consistent with molecular mechanics formulations. The results demonstrate that the Euler beam model overestimates the values of natural frequencies.

Keywords: Carbon nanotubes, eigenfrequency, Euler beam model, shell model, numerical modeling.

1. Introduction

Recent studies have indicated that carbon nanotubes (CNTs) exhibit superior mechanical and electronic properties over any known materials. Due to their novel electronic, mechanical and other physical and chemical properties, CNTs have potential applications in atomic–force microscopes, field emitters, nanoactuators, nanomotors, nanbearings, nanosprings, nanofillers for composite materials, and nanoscale electronic devices. Hence, carbon nanotubes (CNTs) have become the focal points of studies in computational nanomechanics and computational condensed-matter physics over the recent years, including vibrational behavior. Since controlled experiments at the nanometer scale are very difficult, two approaches are widely used for the researches on CNTs. One is the molecular dynamics simulations which is very time-consuming and remains formidable for large–scale systems. The other is the continuum mechanics methods such as shell and beam modeling of CNTs. Via nanotechnology, the nonlocal theory has been applied to analyze vibration and

wave propagation of CNTs based on the beam models [1–5], including also the non-linear interaction with the surrounding medium [6]. Ru [7-8] used the elastic shell model to conduct buckling analyses of CNTs. Yakobson et al. [9] noticed the unique features of fullerenes and developed a continuum shell model to study different instability patterns of CNTs under different compressive loads. He et al. [10-13] investigated the buckling behavior of CNTs using elastic shell model having the van der Waals effect. Muc [14] discussed the applicability of thin shell theory in predicting behavior of CNTs.

In contrast to theoretical considerations the experimental verifications of the CNTs strength or Young's modulus demonstrate evidently discrepancies that may reach even up to 30% - see e.g. Mielke *et al.* [15]. Possible single or multiple defects in CNTs provide an explanation for the extant theoretical–experimental differences.

However, this deterioration in the mechanical characteristics is partly alleviated by the ability of nanotubes to heal vacancies in the atomic network by saturating dangling bonds. The defects can appear at the stage of CNTs growth and purification, or later on during device or composite production. Moreover, defects in CNTs can deliberately be created by chemical treatment or by irradiation to achieve the desired functionality. Therefore, possible defects in CNTs can be classified in the following manner: 1) point defects such as vacancies, 2) topological defects caused by forming pentagons and heptagons e.g. 5-7-7-5 defect – so-called Stone-Wales defects, 3) hybridization defects due to functionalization. It is possible to consider single walled CNTs (SWCNTs) with a single vacancy (one atom removed), with a double vacancy (two adjacent atoms knocked out) and with a triple vacancy (three adjacent atoms missing), as depicted in Fig. 1. In what follows, these configurations will be referred to as non–reconstructed defects. In each tube the non–reconstructed double vacancy defects have two axially distinguishable orientations separated by 120 degrees (only one configuration is shown in Fig. 1). These atomic configurations are metastable but can survive for macroscopic times at low temperatures or when the atoms with dangling bonds are bonded to a surrounding medium, e.g., a polymer matrix.

In this study the axial vibrations of SWCNTs are analyzed only. The free vibrations are investigated with the use of three different models:

- the Euler beam model,
- the continuous specially orthotropic cylindrical shell model,
- the 3-D FE beam model based on the molecular dynamic and the interatomic potential formulations.

The numerical results are presented for one nanostructure configuration only; however, they can be easily extended for other form of structures. The lack of appropriate material properties is especially emphasized.

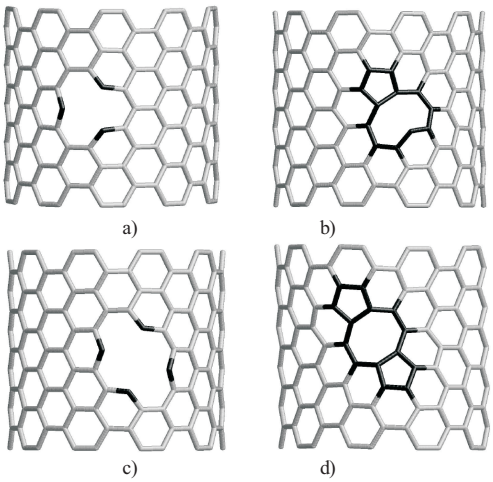

Figure 1 Atomic networks of SWCNTs with non–reconstructed (a, c) and reconstructed (b, d) single (a, b) and double (c, d) vacancy. Only the front wall of each tube is shown. The configurations correspond to (10,10) armchair SWCNT

2. Free Vibrations of Pristine CNTs

A single–walled carbon nanotube can be defined as a hollow cylinder rolled from a graphene sheet. The nanotube, composed of carbon hexagons, is indexed by a pair of integers ($n1$, $n2$) to represent its helicity. The radius of the nanotube is calculated as:

$$R = a\sqrt{3\,(n1^2 + n2^2 + n1n2)}/\,(2\pi) \tag{1}$$

where $a = 0.142$ [nm] is the C–C bond length. One type of nanotubes, armchair ($n1 = n2$, i.e. $R = 0.0678{*}n1$ [nm]) is studied in this paper.

In the literature it is demonstrated that for small radius of the nanotubes the buckling mode falls into the regime of Euler beam buckling (R $<$ 0.8 [nm]) and then with the increase of the radius the circumferential modes of buckling (i.e. for n $>$ 1) becomes to be dominant. Therefore the analytical studies are limited to the axisymmetric buckling/vibration analysis only, i.e. $n = 0$ and $m > 0$. For simply supported cylindrical shells (Fig. 2) made of a specially orthotropic material the eigenfrequencies can be easily derived in the analytical way using the Rayleigh–Ritz method as the roots of the following equation:

$$\psi^3 + b_0\psi^2 + c_0\psi - d_0 = 0 \tag{2}$$

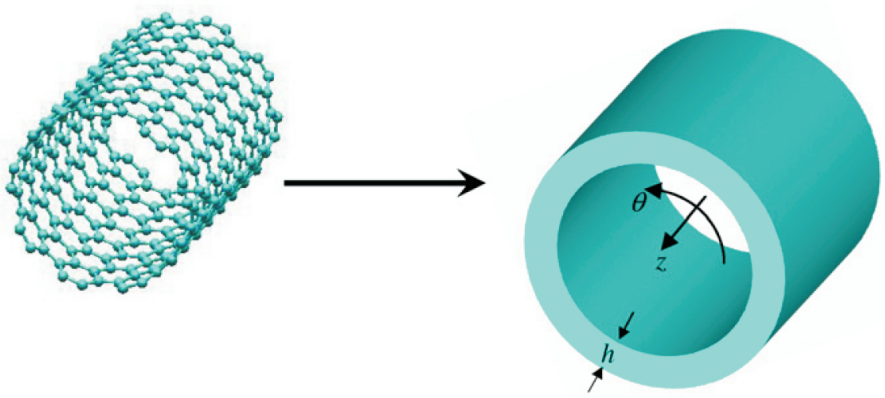

Figure 2 A cylindrical shell equivalent in mechanical response to a SWCNT

where:

$$\begin{aligned} b_0 &= -a_{11} - a_{22} - a_{33} \qquad c_0 = a_{11}a_{22} + a_{11}a_{33} + a_{22}a_{33} - a_{13}^2 \\ d_0 &= a_{11}a_{22}a_{33} - a_{22}a_{13}^2 \qquad a_{11} = \lambda_m^2 \\ a_{22} &= \frac{A_{66}}{A_{11}}\lambda_m^2 \qquad a_{33} = \frac{A_{22}}{A_{11}} + \frac{h^2}{12R^2}\lambda_m^4 \\ a_{13} &= -\frac{A_{12}}{A_{11}}\lambda_m \qquad \lambda_m = \frac{m\pi R}{L} \qquad \psi = \rho R^2 h\omega 2/A_{11} \end{aligned} \tag{3}$$

ρ, R, h and L denote the nanotube density, radius, equivalent thickness and length, respectively, and m, n are wavenumbers in the longitudinal and circumferential directions. A_{ij} are the membrane stiffness matrix coefficients for specially orthotropic bodies. The roots of Eq. (2) can be represented as follows:

$$\psi_1 = a_{22}, \ \psi_{2,3} = \frac{1}{2}\left(a_{11} + a_{33} \pm \sqrt{a_{11}^2 + 4a_{13}^2 - 2a_{11}a_{33} + a_{33}^2}\right) \tag{4}$$

If the carbon nanotube arrays are assumed to be transversely isotropic the material properties in the circumferential and thickness directions are identical. However, the twisted array SWCN is a helical array then, in fact, the nanotube does not possesses completely transversely isotropic properties. Therefore five material constants are necessary to characterize the CNT array behavior. Using micromechanical approach Popov et al. [16] computed four of them, and Salvatat et al. [17] gave the fifth material constants (G_{23}). The values of constants take the following form: E_1 = 580 [GPa], $E_2 = E_3$= 9.4 [GPa], $\nu_{12} = \nu_{13}$ = 0.18, ν_{23} = 0.90, $G_{12} = G_{13}$ = 17.2 [GPa], G_{23} = 2.47 [GPa]. The direction denoted by "1" corresponds to the longitudinal one. In addition let us assume ρ = 600 [kg/m^3] and L = 29.5 [nm]. Thus, for $\psi = 1$ the square root of the ratio $A_{11}/(\rho h R^2)$ is equal to 6.55 [THz] ($n1 = n2 = 5$) and is the multiplier of natural frequencies – Eq. (3). As it may be

seen the magnitude of natural frequencies (THz) is in the range mentioned in the literature. For ($5 = n1$, $5 = n2$) carbon nanotubes the radius $R = 0.339$ [nm] the parameter $\lambda_m = 0.0314{*}m$ and it is treated as negligibly small. Since all membrane stiffnesses A_{ii} are proportional to the thickness parameter h so that that constant can be omitted in the further considerations.

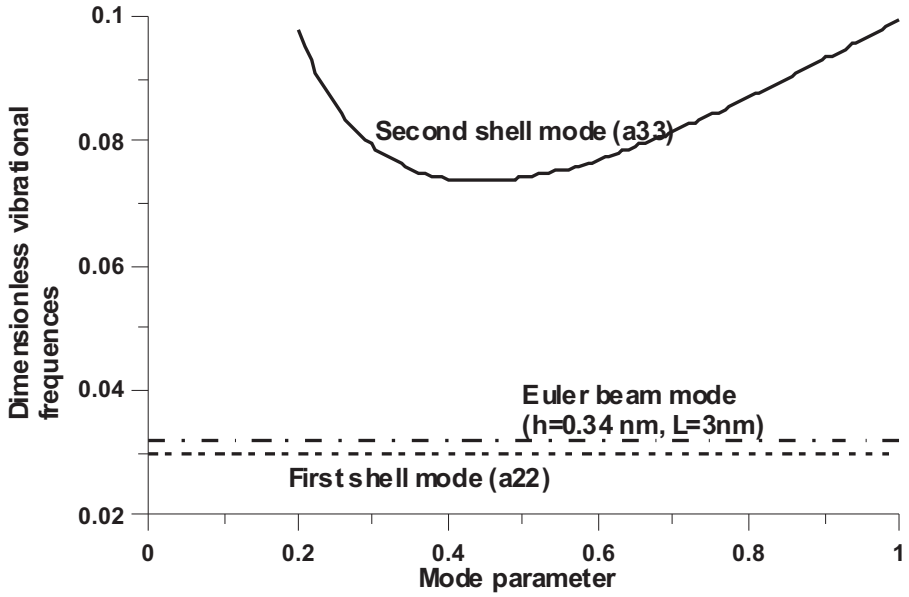

Figure 3 Comparison of vibrational frequencies for different models

Fig. 3 demonstrates the comparison of the values of the frequencies described by Eq. (4) and the value corresponding to the Euler beam model which is given by the relation:

$$\psi_{Euler} = \left(m\pi\frac{h}{L}\right)^2 \lambda_m^2 \tag{5}$$

In Fig. 3 the x axis corresponds to the value λ_m^2 and the y axis represents the valueψ/λ_m^2. As it may be easily noticed from the relations (4) the first shell mode is constant and equal to a_{22}/λ_m^2, the second – a_{33}/λ_m^2 and the third (not plotted in Fig. 3) is equal to a_{11}/λ_m^2 so that is equal to 1. It is necessary to emphasize that the above formulas are the approximations only for the second and the third modes but they are satisfactory for the present numerical data. In the second shell mode and in the Euler beam model the shell thickness h is equal to 0.34 [nm]. In the plot the first shell mode corresponds to the lowest frequency. It is worth to mention also that in the literature the frequencies are usually compared with values obtained with the use of the Euler beam model. However, the use of the shell model allows us to predict lower value but the relation between those values is strongly dependent on the assumed CNT length L. For higher values the Euler value can be lower than that corresponding to the application of the shell model.

3. Reconstruction of Vacancies – Evaluation of Free Vibrations

Now, the eigenfrequency analysis will be adapted to the estimations of free vibrations for defective nanotubes. The reconstruction of the defective structure can be modeled in two ways:

- the new positions of the carbon atoms are derived in order to keep the form plotted in Figs 1.b and 1.d; in such a case the distances between C-C bonds are constant and equal to 1.42 [nm] should be shifted below the pristine shell structure;

- the new position are derived from the condition of the minimal energy for neighborhood atoms; in such a situation it is necessary to introduce the interaction potential – see Muc [14, 18].

In the present analysis the first simplest method is used. The key difference in the comparison with other works is that the former bear on the intrinsic material property (bond strength), whereas the proposed method relates to tube geometry. It should be noted that the present analysis relies a continuum representation of nanotubes. Since atomic scale kinematics is not considered, the analysis may tend to over predict the eigenfrequencies of structures.

Let us consider the defective carbon nanostructure as the space–frame structure where each of the C–C bonds is represented as a beam. The stiffness of the C–C bond is variable but at the beginning of the deformation process it is equal to 1 [TPa]. Then, it is evaluated incrementally at each step of deformations with the aid of the Tersoff-Brenner potential. It is assumed that in the carbon nanostructure each carbon atom may react with the neighborhood atoms only. As the atom moves from the equilibrium state the non-zero reaction force is computed as the first derivative of the potential. We restrict the motion of the two atoms to one dimension, along the line connecting them, so that the atoms can only move directly towards or away from one another. It is necessary to point out that the C–C bond stiffness is not equal to the stiffness moduli mentioned in the previous section since they characterize the properties of the whole nanotube shell.

The numerical space–frame model of carbon nanotubes is presented in Fig. 4. One of the ends of the tube is simply supported, whereas at the second the symmetry conditions are imposed. The carbon nanotubes remain cylindrical until the critical eigenfrequency is reached at which point they deform in the longitudinal direction (i.e. $n = 0$). The half of nanotubes is modeled only due to symmetric boundary conditions. The natural frequencies have been obtained with the use of the NISA FE package.

Fig. 5 represents the differences in the first two eigenfreuquencies for defective and pristine carbon nanotubes derived with the use of the beam model. The analysis was carried out for two form of vacancies plotted in Fig. 1 and two modes of eigenfrequencies corresponding to $m = 1$ and $m = 2$. The numerical model shows the classical situation of the frequency decrease with the increase of the number of vacancies. The differences reach almost 10%.

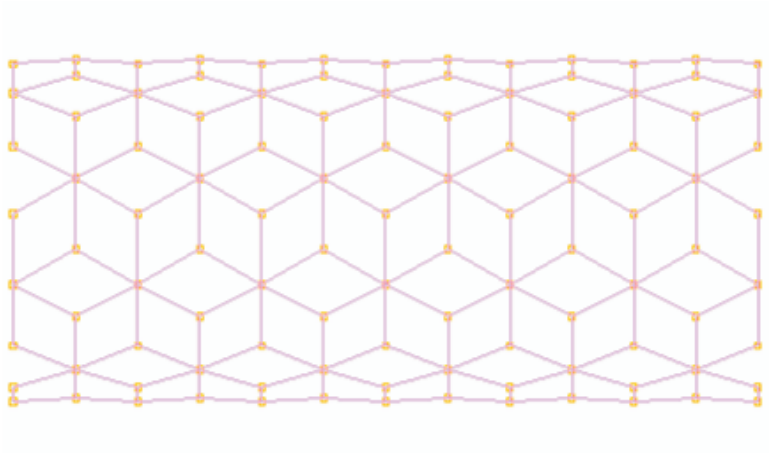

Figure 4 Numerical model of the (5,5) carbon nanotube

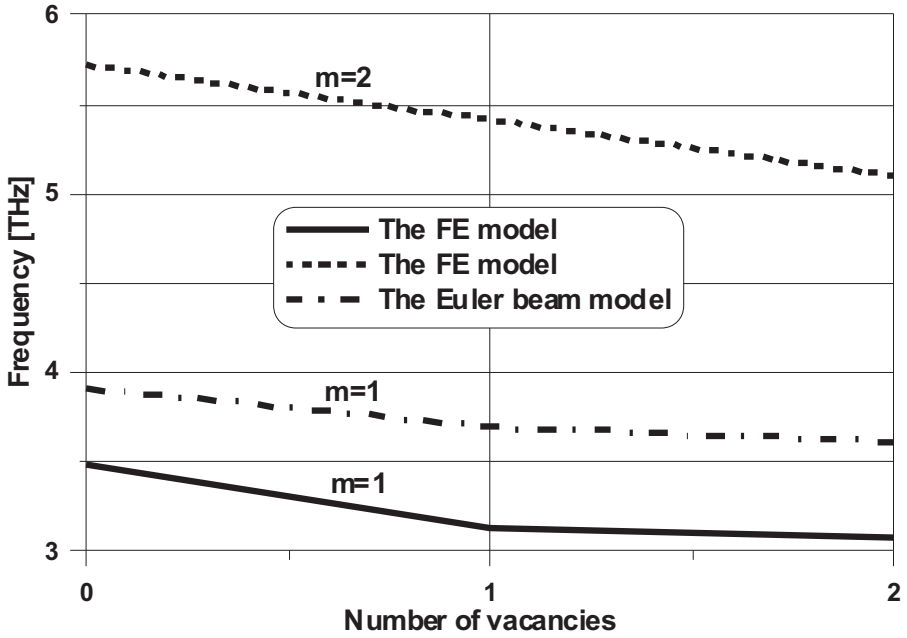

Figure 5 Frequency as a function of the number of vacancies

4. Stress–Strain Curves

Using the FE model it is also possible to plot the stress–strain curves for the pristine and defective nanostructures. In our approach (see Muc [19]) the Young's modulus of a material is defined as the ratio of longitudinal stress to longitudinal strain as obtained from a uniaxial tension test. Following this definition, the Young's modulus of CNTs is been calculated using the following equation:

$$E_{long} = \frac{\langle \sigma_{long} \rangle}{\langle \varepsilon_{long} \rangle}, \quad \langle \sigma_{long} \rangle = \sum_{k=1}^{N_{beams}} \sigma_{long}^{k}, \quad \langle \varepsilon_{long} \rangle = \sum_{k=1}^{N_{beams}} \varepsilon_{long}^{k} \tag{6}$$

where $\langle \sigma_{long} \rangle / \langle \varepsilon_{long} \rangle$ is an average longitudinal stress/strain component computed as the sum of longitudinal components of each individual beams characterizing C–C bonds. Let us note that the above definition is more general than that described as the global on in the first section and it is consistent with the homogenization theory. At each load step corresponding to the increments of the axial displacements, the molecular mechanics force field constants as well as the beam geometrical and mechanical properties are evaluated in order to find the longitudinal stress components in individual beams. This iterative, non–linear procedure goes on to the prescribed end of the deformation process. The accuracy of modeling procedure depends on the number of load steps chosen. In order to maximize the accuracy of computational results, in each case, the displacement increment was chosen from convergence tests in which the convergence criterion was set equal to 2% of the maximal stress. Thereby, if between two sequential displacement increments a difference smaller than the 2% was achieved in the computed maximal stress, the larger displacement increment was finally adopted for the analysis.

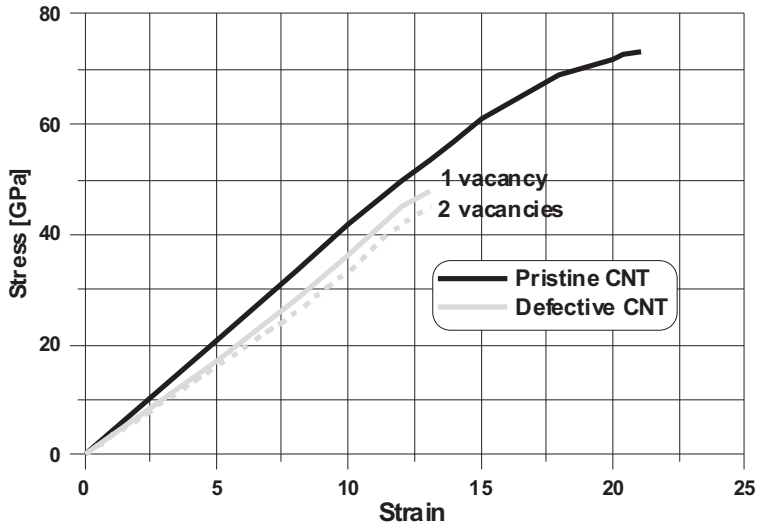

Figure 6 Tensile stress–strain curves for pristine and defective (5,5) nanotube

Fig. 6 shows the calculated stress–strain curves and Young's modulus of pristine and defective (with one–atom vacancy) carbon nanotubes from the present models. At the beginning we have compared the Young's moduli of (5, 5) armchair CNTs. The predicted initial Young's modulus of CNTs are 797 [GPa], 708 [GPa] and 682 [GPa] for the pristine and defective CNT with one and two vacancies (Fig. 1), respectively, which agrees well with the experimental value and other theoretical values mentioned previously. Those values are strongly dependent on the form of the assumed interatomic potential and the form of defects. The defects reduce the failure stresses by 19%, and failure strains by 32%. It may reduce also buckling stresses for compressive loads since the defect considered may be treated as a geometrical imperfection for cylindrical shells. It is also obvious that the reduction factor is significantly dependent on the form and magnitude of imperfections (the assumed type of defects).

For the estimated values of Young's moduli it is possible to find the eigenfrequencies. Since in the present analysis the longitudinal Young modulus is known only the values of frequencies are computed with the aim of the Euler beam model Eq. (5). The results are plotted in Fig. 5. Using that relation it can be easily derived that:

$$\frac{\omega\,(m=2)}{\omega\,(m=1)} = 4 \text{ if E identical } \frac{\omega_{pristine}}{\omega_{defective}} = \sqrt{\frac{\mathrm{E}_{pristine}}{\mathrm{E}_{defective}}} \tag{7}$$

As it may be seen in Fig. 5 the Euler beam estimations of eigenfrequencies is not correct since it gives higher values that the FE beam model. In addition, the differences between values for the neighbourhood wavenumbers ($m = 1$ and $m = 2$) are also too high – Eq. $(7)_1$. On the other hand, the comparison of the frequencies for pristine and defective nanotubes is much better – Eq. $(7)_2$.

5. Conclusions

We have used three different models (the Euler beam model, the continuous shell model and the FE model) to study axial free vibrations of the configuration of a single-walled carbon nanotube with and without vacancy defects. It is found that the best description of eigenfrequencies can be obtained with the use of the numerical FE model. However, that model should be enriched by the appropriate material models taking into account transversely isotropic properties of nanostructures.

There is a significant difference in natural frequencies for the pristine and defective nanostructures. In view of that it is possible to use one of the most quantitative non–destructive testing (NDT) techniques, ultrasonic NDT to distinguish defective SWCNTs. Today it has been much progress in instrument technology so that it will be possible to find testing techniques able to reveal anomalies in the material property.

Acknowledgements

The Polish Research Foundation PB 1174/B/T02/2009/36 is gratefully acknowledged for financial support.

References

[1] **Zhang, Y. Q., Liu, G. R. and Xie, X. Y.**: Free transverse vibration of double–walled carbon nanotubes using a theory of nonlocal elasticity, *Phys. Rev. B*, 71, 195404–195407, **2005**.

[2] **Wang, Q. and Varadan, V. K.**: Vibration of carbon nanotubes studied using nonlocal continuum mechanics, *Smart Mater. Struct.,* 15(2), 659–666, **2006**.

[3] **Wang, Q., Zhou, G. Y. and Lin, K. C.**: Scale effect on wave propagation of double–walled carbon nanotubes, *Int. J. Solids Struct.,* 43(20), 6071–6084, **2006**.

[4] **Hu, Y. G., Liew, K. M. and Wang, Q.**: Nonlocal elastic beam models for flexural wave propagation of double-walled carbon nanotubes, *J. Appl. Phys.,* 106(4), 044301–044306, **2009**.

[5] **Ke, L. L., Xiang, Y., Yang, J. and Kitipornchai S.**: Nonlinear free vibration of embedded double-walled carbon nanotubes based on nonlocal Timoshenko beam theory, *Comput. Mater. Sci.*, 47(2), 409–417, **2009**.

[6] **Mustapha, K. B. and Zhong, Z. W.**: Free transverse vibration of an axially loaded non–prismatic single–walled carbon nanotube embedded in a two–parameter elastic medium, *Comput. Mater. Sci.*, 50(2), 742–751, **2010**.

[7] **Ru, C. Q.**: Effective bending stiffness of carbon nanotubes, *Phys. Rev. B*, 62(15), 9973–9976, **2000**.

[8] **Ru, C. Q.**: Elastic buckling of single–walled carbon nanotube ropes under high pressure, *Phys. Rev. B*, 62(15), 10405–10408, **2000**.

[9] **Yakobson, B. I., Brabec, C. J. and Bernholc, J.**: Nanomechanics of carbon tubes: instabilities beyond linear range, *Phys. Rev. Lett.,* 76(14), 2511–2514, **1996**.

[10] **He, X. Q., Kitiporchai, S. and Liew, K. M.**: Buckling analysis of multi-walled carbon nanotubes: a continuum model accounting for van der Waals interaction, *J. Mech. Phys. Solids,* 53(2), 303–326, **2005**.

[11] **He, X. Q., Kitipornchai, S., Wang, C. M. and Liew, K. M.**: Modeling of van der Waals force for infinitesimal deformation of multi-walled carbon nanotubes treated as cylindrical shells, *Int. J. Solids Struct.*, 42(23), 6032–6047, **2005**.

[12] **Kitipornchai, S., He, X. Q. and Liew, K. M.**: Buckling analysis of triple-walled carbon nanotubes embedded in an elastic matrix, *J. Appl. Phys.,* 97(11), 114318–7, **2005**.

[13] **Liew, K. M., He, X. Q. and Kitipornchai, S.**: Buckling characteristics of embedded multi–walled carbon nanotubes, *Proc. R. Soc. A*, 461(2064), 3785–3805, **2005**.

[14] **Muc, A.**: Modeling of carbon nanotubes behaviour with the use of a thin shell theory, *J. Theor. Appl. Mech.*, 49(2), 531–540, **2011**.

[15] **Mielke, S. L., Troya, D., Zhang, S., Li, J. L., Xiao, S., Car, R., Ruoff, R. S., Schatz, G. C. and Belytschko, T.**: The role of vacancy defects and holes in the fracture of carbon nanotubes, *Chem. Phys. Lett.,* 390(4–6), 413–420, **2004**.

[16] **Popov, V. N., Van Doren, V. E. and Balkanski, M.**: Elastic properties of crystals of carbon nanotubes, *Sol. Stat. Comm.*, 114(7), 395–399, **2000**.

[17] **Salvetat, J. P., Briggs, G. A. D., Bonard, J. M., Bacsa, R. R., Kulik, A. J., Stockli, T., Burnham, N. A. and Forro, L.**: Elastic and shear moduli of single–walled carbon nanotube ropes, *Phys. Rev. Lett.,* 82(5), 944–947, **1999**.

[18] **Muc, A.**: Design and identification methods of effective mechanical properties for carbon nanotubes, *Mat. Des.,* 31(4), 1671–1675, **2010**.

[19] **Muc, A.**: Modeling of CNTs/nanocomposites deformations and tensile fracture, *Proc. 17th Int. Conf. Compos. Mat. (ICCM17)*, 1–9, **2009**.